

Atmosphere

Volume 11 Number 1 1973

Canadian Meteorological Society
Société Météorologique du Canada

Atmosphere

Volume 11 Number 1 1973

Contents

1

Mesoscale Effects of Hailstorms on the Environmental Air
N.J. Cherry and R.R. Rogers

13

The Pseudospectral Approximation Applied to the
Shallow Water Equations on a Sphere
Philip E. Merilees

20

Book Reviews

21

A Case Study of Mixing-Height Variations
in the Toronto Area
B. Padmanabhamurty and R.E. Munn

26

A Note on Waves, Wavegroups, and Local Influence
James H.S. Bradley

30

Notes from Council

31

A Mirage at Regina
John R. Hendricks

33

Announcement

Mesoscale Effects of Hailstorms on the Environmental Air

N.J. Cherry and R.R. Rogers

Department of Meteorology, McGill University, Montreal

[Manuscript received 20 October 1972; revised 10 March 1973]

ABSTRACT

Serial radiosonde ascents from Penhold, Alberta for four storm days were analyzed to study the variations in height and time of the temperature, potential temperature (dry and wet-bulb), moisture, convective stability, and wind velocity. This information was compared with previous analyses of the storm activity on these days. It was found that the storms had little effect on the ambient temperature field but showed a marked effect on the moisture field. Convective instability, that existed at low levels before the storm activity, was greatly re-

duced in the air behind the storms. The variability of the field of wet-bulb potential temperature shows that radiosondes released more than about two hours in advance of a storm were unrepresentative of the conditions near the storm. An elementary one-dimensional updraft model was applied to parcels of air from below the second significant level (i.e., below about 300–500 m AGL), assuming the air to be completely mixed. The model gave vertical velocity profiles that were in qualitative agreement with those in the observed storms.

1 Introduction

A number of one-dimensional storm models have been developed during the past few years which are variously used in forecasting (Chisholm, 1970), in the planning and assessment of cloud modification experiments (Weinstein and Davis, 1968; Simpson, 1971), and in theoretical studies of precipitation development (Danielsen *et al.*, 1972). Some of these models account for complex dynamic, thermodynamic, and microphysical processes; others are not far removed from classical parcel theory. The primary input data to each of the models, regardless of its complexity, consist of an ambient atmospheric sounding of temperature and humidity. In practice it is often necessary to rely on a sounding obtained remotely in time and space from the storm to describe its ambient conditions. A question then naturally arises about the representativeness of remote soundings for characterizing the environment of a storm.

Cloudy convection brings about the conversion of potential to kinetic energy and the change in phase of water substance. A storm thus interacts with its environment and will modify the thermodynamic properties of the air, at least locally. Questions arise about the extent and intensity of these storm-environment interactions.

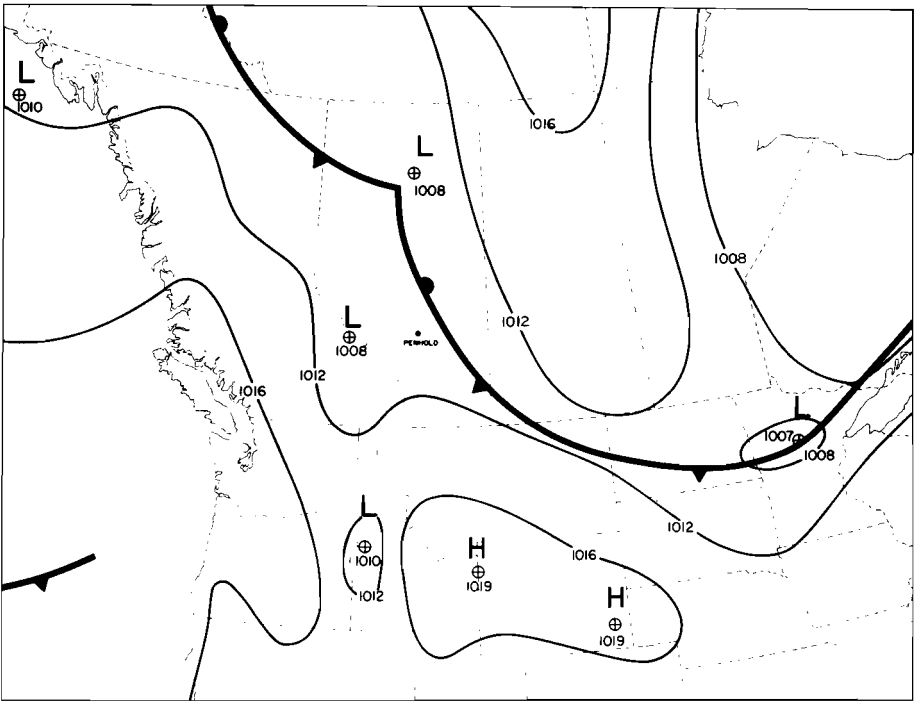


Fig. 1a Surface chart for 1700 MST 28 July 1967.

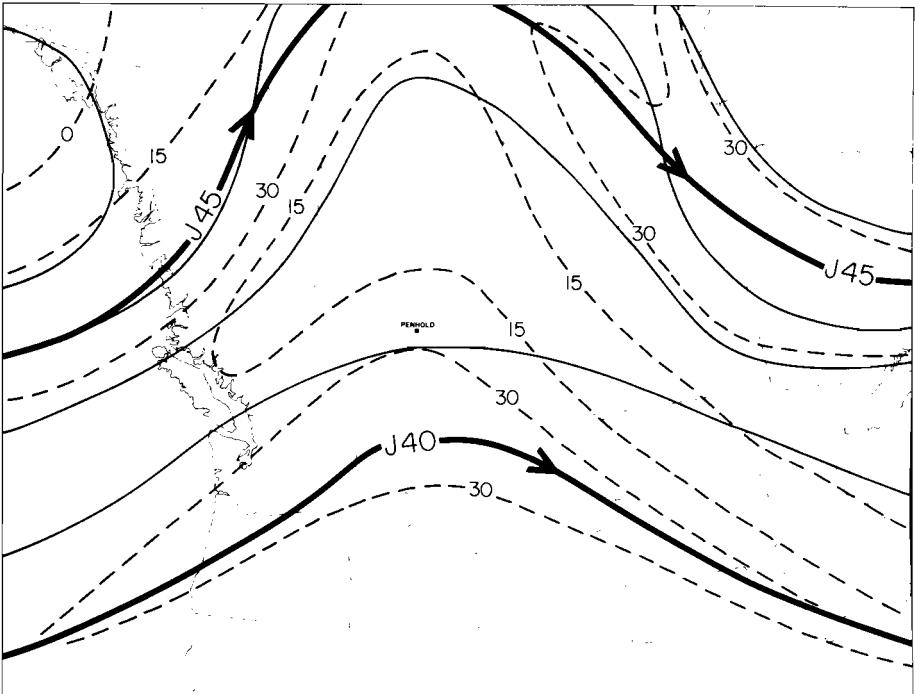


Fig. 1b 300-mb chart for 1700 MST 28 July 1967. The broad lines show the positions of the upper level jets. The narrow solid lines are contours of geopotential height and the broken lines are isotachs. All speeds are given in m s^{-1} .

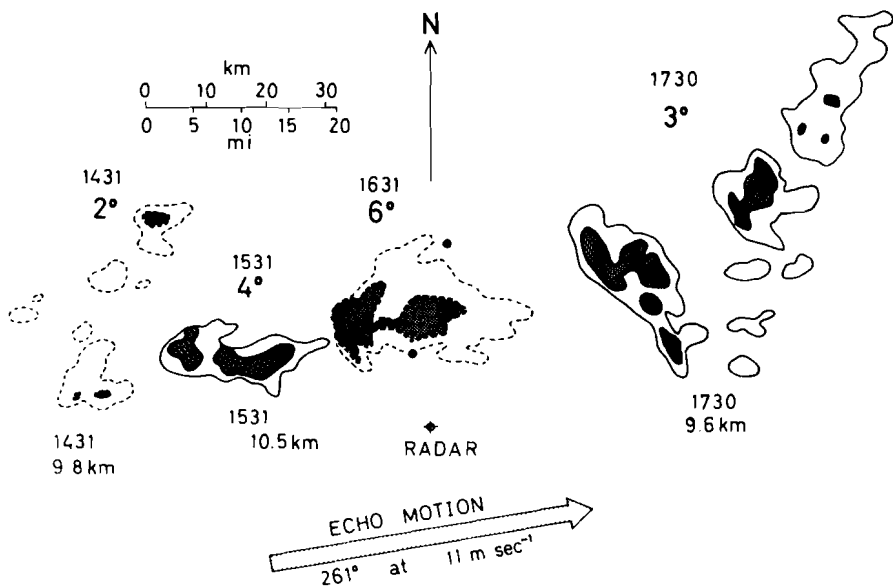


Fig. 1c PPI sections at four different times between 1431 and 1730 MST on 28 July 1967. The height above ground of the radar echo top is indicated below each section and the elevation angle of the PPI is given above. Light shading denotes reflectivities of shade 1 and greater and dark shading indicates reflectivities greater than shade 3. (From Ragette, 1973.)

On some occasions when hailstorms were being observed by radar within the project area of the Alberta Hail Studies Project* radiosondes were released in sequence from the radar site at intervals of between one and two hours. The series usually commenced in the late morning and continued until the evening. These serial ascents have been analyzed in an attempt to answer questions about the representativeness of remote soundings and the interaction between storm and environment.

2 Discussion of the observations

Data were analyzed from four days on which there were serial radiosonde releases. Of these, the two cases with more complete data coverage were studied in detail and are presented here. General conclusions given later apply to all four cases which involve air mass storms.

a 28 July 1967

The synoptic situation on 28 July 1967 is illustrated by the charts in Figs. 1a and 1b. The surface chart shows a front which moved through southern Alberta on the morning of 28 July. The associated low level winds were light and from the northwest, a situation which was still in evidence late the next

*ALHAS is a joint research program of the Alberta Research Council, National Research Council, Atmospheric Environment Service, and McGill University.

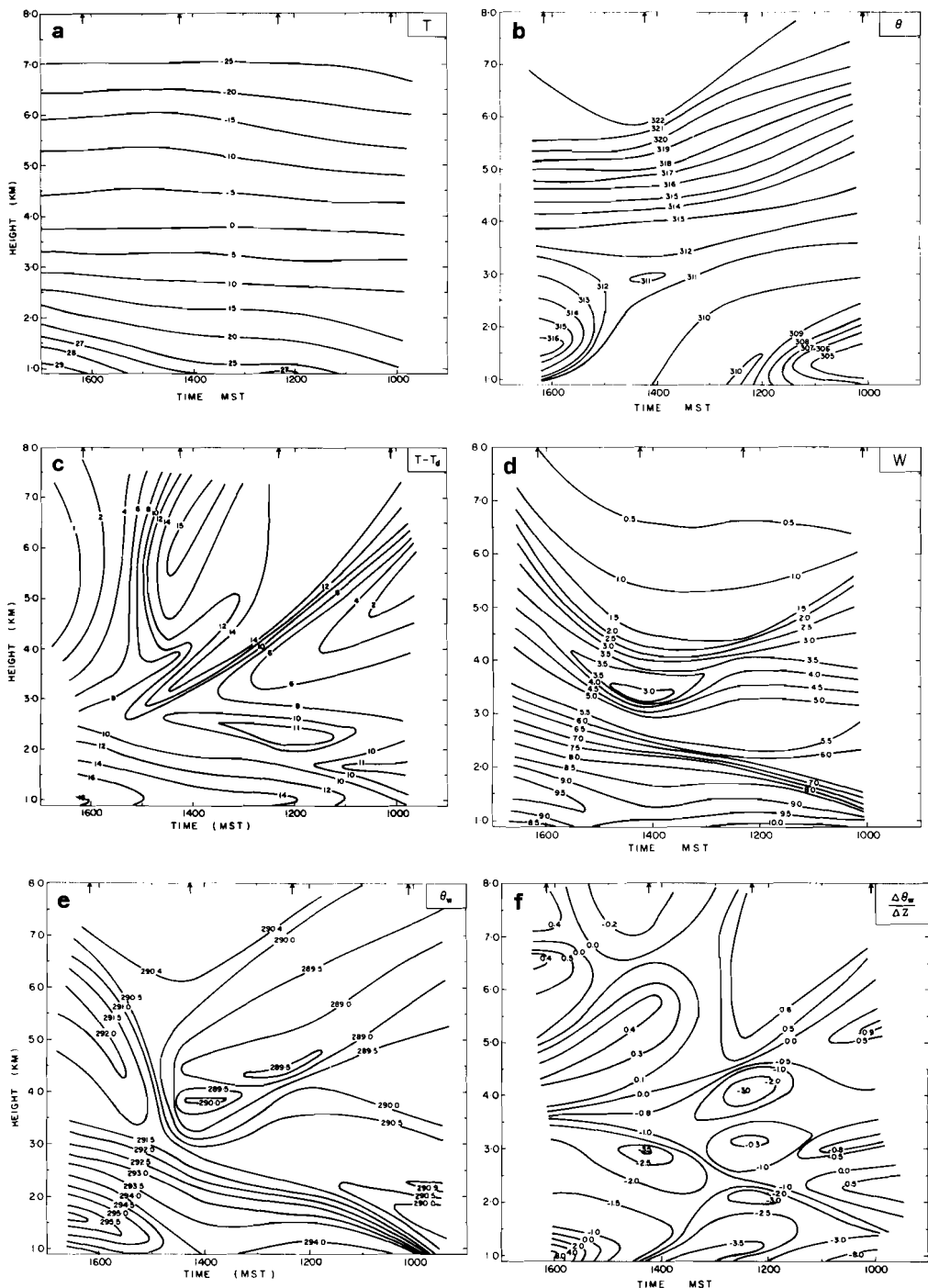


Fig. 2 Time-height profiles for 28 July 1967. Arrows along the upper scale indicate radiosonde release times. (a) temperature ($^{\circ}\text{C}$), (b) potential temperature (K), (c) dew-point depression (K), (d) mixing ratio (g kg^{-1}), (e) wet-bulb potential temperature (K), (f) convective instability (K km^{-1}).

day when the front had moved slowly eastward to lie diagonally across Saskatchewan by noon. The 300-mb chart shows a west to southwest flow over Penhold at about 20 m s^{-1} . The jet to the south moved northwards, weakening slowly, such that it was directly over Penhold by 0500 MST 29 July, with a wind speed of about 35 m s^{-1} .

Fig. 1c illustrates the radar structure of the storm of 28 July at successive times between 1431 and 1730 MST. At about 1630, while in its mature stage, the storm passed within 13 km of the radar site, as shown. This storm was studied by Ragette (1973) and others, who described it as a supercell (quasi steady-state) storm during its peak-development period.

Fig. 2a is an analysis of the temperature field in time-height coordinates, based on data from four serial ascents. The radiosonde release times are indicated by the arrows along the top of the diagram, the last one being just after 1600 and shortly before storm passage. The time scale is reversed to assist in relating the pattern to storm activity by approximating a flow from left to right. The temperature field shows the effect of surface heating, which decreased with height and was negligible at the 0°C level.

The dry air potential temperature, Fig. 2b, shows that the air below 4 km generally had close to neutral static stability. It was unstable near the surface at 1000 and between 1.5 km and 3.5 km at 1600. Above 4 km the air was quite stable, though with an indication that the stability decreased above 6 km at 1600.

Fig. 2c shows the dew-point depression, which is related inversely to the relative humidity. The air below 3 km was relatively dry. Moist air aloft at 1000 was replaced by dry air by midday. Later in the afternoon the moisture in the upper air increased very rapidly. The mixing ratio, Fig. 2d, indicates that the air at the surface became drier during the afternoon. After 1400 the mixing ratio increased with time at all levels above 2 km.

The wet-bulb potential temperature, θ_w , was computed as a function of altitude for each sounding and is analyzed in Fig. 2e. Henderson (1971) related isotherms of θ_w to parcel trajectories using the fact that this quantity is conserved for a parcel which does not mix with the surrounding air. This conservative property will tend to confine parcels to surfaces of constant θ_w . Henderson was assisted in his study by the fact that the wind direction changed little with height. When directional shear is present (as in the present case) parcels will not remain in a plane. Then a diagram such as Fig. 2e cannot be used to depict trajectories.

The θ_w profile given by each radiosonde was differentiated with respect to height to determine the convective stability of the air, Fig. 2f. Where $\Delta\theta_w/\Delta z$ is negative the air is called convectively unstable; where it is zero the air is convectively neutral; and where it is positive the air is called convectively stable. Fig. 2f shows increasing convective instability at most levels below 4 km as the day progressed, up until about 1400, after which the lowest levels rapidly became more stable.

The wind speed, Fig. 3a, generally decreased with height in the lower layers,

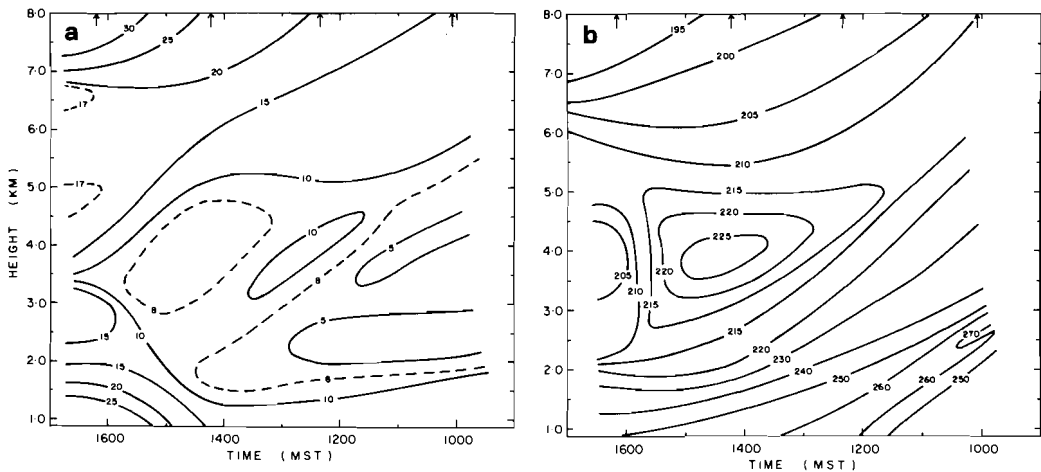


Fig. 3 Time-height profiles for 28 July 1967. (a) wind speed (m s^{-1}), (b) wind direction (deg).

was approximately constant in the middle layers, and increased with height above about 5 km. By 1600 the wind speed increased and showed increased variability with height. The wind direction, Fig. 3b, shows a general swing towards the south both in height and time.

b 29 July 1967

On this day five radiosondes were released at intervals of approximately two hours, the final one being after the storms had passed. Three distinct storm cells were observed on the radar (Warner *et al.*, 1972). The first developed at 1330 MST 70 km from the radar in the direction 240° . It travelled approximately from the southwest and dissipated at about 1430. The main storm was large and long-lived. It developed about 100 km west of the radar at 1400 and travelled along a path from a few degrees north of west at a speed of about 5 m s^{-1} . Its anvil was over the radar by about 1630 and the bulk of the storm dissipated as it approached the radar at 1730. A third storm formed behind the main storm at 1600 and followed along the same track, crossing the radar in its mature stage between 1800 and 1900. The 1819 radiosonde ascended through the north side of this storm.

As in the case of 28 July the temperature field, Fig. 4a, shows little variation in time except near the surface where diurnal heating is evident. The field of dry-air potential temperature (not shown) was also similar to the 28 July case in that the air below 4 km was unstable or had close to neutral static stability. After 1800 the air near the surface became very stable as a consequence of surface cooling.

The dew-point depression field, Fig. 4b, shows that between 1200 and 1400 the air was relatively moist at low levels and dry above. By 1700 the situation was reversed. After 1800 the air near the surface was quite moist. Fig. 4bi is an approximate north-south cross section using the 1700 radiosonde from

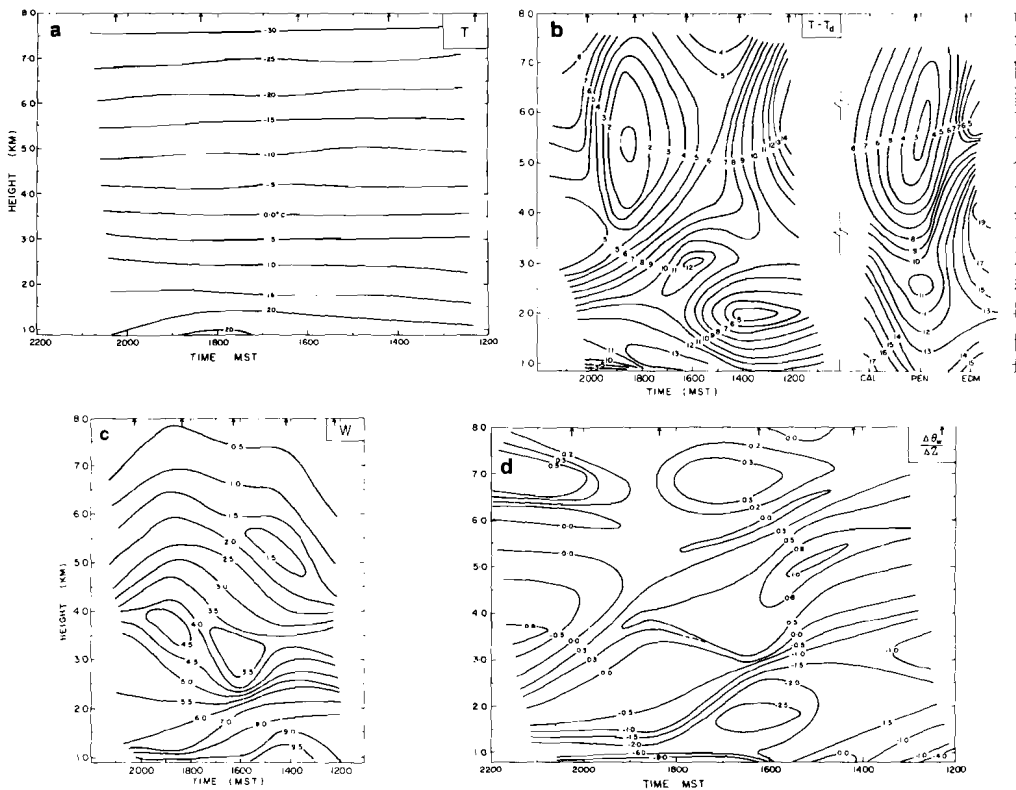


Fig. 4 Time-height profiles for 29 July 1967. (a) temperature (K), (b) dew-point depression (K). Fig. 4bi, added on the right of this figure, is an approximate north-south cross section of dew-point depression at 1700, included to show the strong space-variability of this field. (c) mixing ratio (g kg^{-1}), (d) convective instability (K km^{-1}).

Edmonton and Calgary and interpolating the Penhold data to 1700. This shows strong variability in the distribution of dew-point depression with distance. The air is quite dry except at upper levels over Penhold and Edmonton.

The derived mixing ratio field, given in Fig. 4c, shows a general decrease of moisture content with height at all times, but a more gradual decrease after about 1700.

Fig. 4d presents the field of convective instability, constructed by differentiating the individual profiles of θ_w with respect to height. It shows that there was initially a convectively unstable layer extending from the surface to about 4.5 km. As the afternoon progressed the depth of the layer decreased and the instability intensified up to about 1600. After this the convective instability generally decreased except for a shallow unstable surface layer. By 2000 the air at all levels above this surface layer had close to neutral convective stability.

Fig. 5a shows the wind-speed field. The wind speed decreased rapidly with height in the lowest kilometre, above which it was fairly constant up to about 5

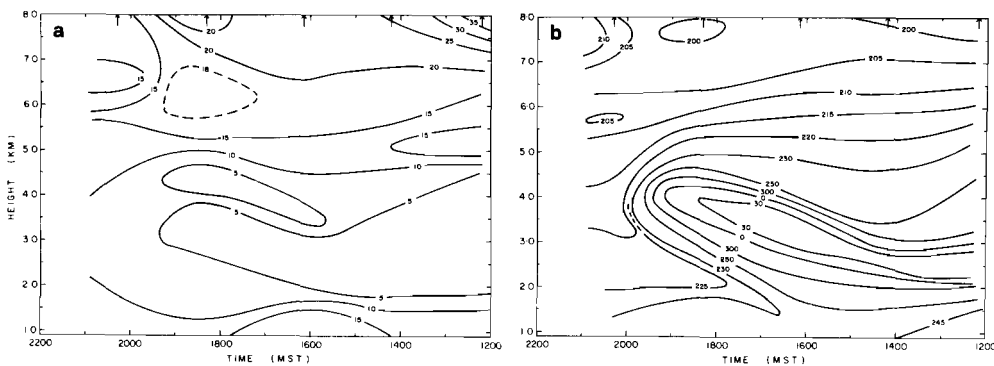


Fig. 5 Time-height profiles for 29 July 1967. (a) wind speed (m s^{-1}), (b) wind direction (deg).

km. Above this level it generally increased. An upper-level jet was observed at 1200, centred at about 8 km. The wind direction is shown in Fig. 5b. Between the surface and about 3 km the wind veered from the southwest to the northwest. Above 5 km the direction varied little with time and backed slowly towards the south with height. After 2000 there was no evidence of the mid-low-level shear.

3 Storm-environment interactions

In addition to the cases of 28 and 29 July, presented in the last section, data from serial ascents on 27 and 29 June 1967 were also analyzed. On three of these days storms passed within 20 km of the radiosonde release site at Penhold. On the remaining day, 27 June, a storm passed 70 km to the south of Penhold. Since the wind was blowing from the northwesterly quadrant at all levels on this day, none of the air from the storm region passed over Penhold or was sensed by the radiosondes. On 29 June and 29 July the coverage was most complete, with radiosondes released in advance of, adjacent to, and behind the storms.

On each of the three days when storms passed close to Penhold little effect was observed on the temperature field in the mesoscale. The moisture field changed markedly, however. The dew-point depression showed that the air quickly approached saturation in the upper levels as the storms neared Penhold. The mixing ratio generally increased at all levels in advance of the storms and decreased behind them.

The air from the surface up to about 4 km above MSL had close to neutral static stability ahead of the storms. The air behind the storms was statically stable throughout the troposphere. Low-level convective instability was present in advance of the storms and was accentuated just before their arrival. The air behind the storms had approximately neutral convective stability except for a shallow, stable surface layer, probably associated with the evaporation of surface water.

The apparent effect of the storms on the airflow was different on each day.

This may be due to a sampling problem. The effective interval in distance between successive radiosondes was large compared to the dimensions of the storms. Therefore the small-scale features of the flow in the immediate vicinity of a storm may or may not have been detected, depending on the proximity of a radiosonde to the storm. In each of the three cases when storms passed close to the station the wind ahead of the storms decreased with height in the first kilometre above the ground. Above this level the speed remained fairly constant for two or three kilometres and then increased with height through the rest of the troposphere. Strong directional shear was present in every case.

4 Representativeness of remote radiosondes

It is very difficult to obtain observations of the environmental conditions of a particular storm unless a special effort is made to do so. The usual practice is to choose the sounding closest in time and space to the storm. How representative this sounding may be depends on the proximity to the storm and whether large-scale shear and vertical motion are present. Shear can lead to differential advection, which will tend to modify the sounding. Vertical motion will also lead to changes in the vertical distributions of temperature and moisture. For example, air moving horizontally at 10 m s^{-1} with an upward velocity of only 10 cm s^{-1} may lead to temperature changes at a given level amounting to about 1°C , depending on the initial temperature profile. The dew point may be changed by more than 1°C , since the variations of dew point with height are usually greater than those of temperature.

From the viewpoints of both storm modelling and forecasting, the most important environmental parameters are the dry- and wet-bulb potential temperatures and their height-derivatives. Observations indicate that these quantities vary smoothly and regularly at times well in advance of storm arrival, but from about an hour and a half to two hours before storm arrival they change in a rapid and relatively unorganized manner. (Examples of these effects are shown in Figs. 2b, 2e, 2f, and 4d.) This time interval, within which the changes become more pronounced, corresponds approximately to the time by which air coming from a storm precedes its arrival at the sounding site.

Thus, data from a radiosonde released $1\frac{1}{2}$ to 2 h in advance of a storm appears to be most representative of the air close to, but unmodified by, the storm. If a sounding is taken to the side of a storm but not downwind, it could be much closer (in time or equivalent distance) without encountering modified air. Fig. 4bi shows, in fact, that a sounding to the side of a storm may need to be within 50 km of the storm to characterize its moisture field accurately.

5 Updraft profiles

Modified parcel theory was applied to the soundings to produce updraft profiles, and these were examined as functions of time. The model is essentially the same as the LMA (Loaded Moist Adiabatic) model of Chisholm (1970), in that the reduction in buoyancy due to the weight of condensed water is taken into account, but no mixing of parcel air with environmental air is considered

after ascent begins. Chisholm found that this model was useful in forecasting convective storms and that it predicted storm tops that agreed closely with radar tops of the largest storms present on a given day.

The buoyancy force per unit mass of air at a given level is

$$F_B = g \left[\frac{T}{T'} - (1 + m) \right] \quad (1)$$

where g is the acceleration due to gravity, T is the virtual temperature of the parcel, T' is the virtual temperature of the ambient air (obtained from the sounding), and m is the mass of condensed water. This force is equated to the parcel acceleration, which is then integrated over height to give the vertical velocity as a function of height,

$$w^2(z) = w_0^2 + 2 \int_{z_0}^z F_B(z) dz \quad (2)$$

where z_0 is the parcel's initial height and w_0 is the vertical velocity at this height. F_B is obtained as a function of height by assuming the parcel ascends dry adiabatically before condensation and moist adiabatically thereafter. The cloud top predicted by this model is z_T , which is the value of z in (2) where $w(z)$ decreases to zero. The second term on the right-hand side of (2), evaluated at z_T , is referred to as the "positive area" and is an index of convective intensity.

The results of this model depend rather critically on the properties of the initial parcel chosen to represent air entering the updraft of the storm. In the calculations the model was applied to unmixed parcels taken from the ambient sounding at the four lowest significant levels, and to parcels obtained by adiabatically mixing air from the lowest two layers and the lowest three layers. The updraft profile calculated for each of these parcels was then compared with the observed cloud base and the echo top, if this information was available. Only parcels from the first significant level above the ground and from the lowest two mixed layers gave results that were consistent with observations. This suggests that air from the surface or from the third significant level or above (i.e., above about 0.7–1 km) is not representative of the air in the storm updraft.

Results based on the mixed parcel from the lowest two layers for two of the days when storms passed close to the observing station are shown in Figs. 6 and 7. The evolution in time of both the updraft profile and the positive area is shown on these diagrams.

Fig. 6, for 29 July, shows a buildup of the available energy (positive area) in the early afternoon to a value of about 0.7 J/g between 1400 and 1600. This energy was evidently released by the storm activity at about 1800, for neither the sounding at 1819 nor at 2017, when used in connection with the model, produced any updraft or positive area. These storms were observed to have radar tops at about 11.5 km, in reasonable agreement with the model results, and produced hail of golf-ball size.

Fig. 7 is for 29 June, on which day a storm passed directly over Penhold at about 1430. Storm tops were at about 8.5 km and bases were at 2.5 km. Hail

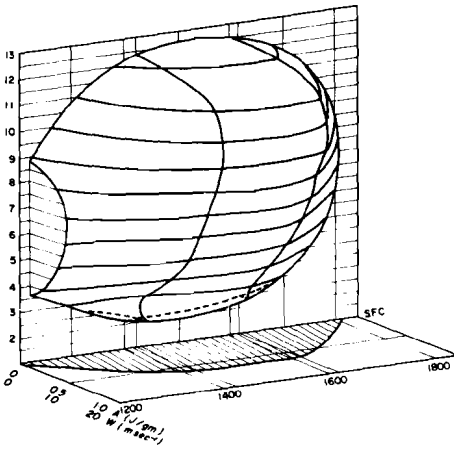


Fig. 6 Vertical profiles of updraft velocity w and positive area A (lower plane) for 29 July 1967 using a one-dimensional updraft model after Chisholm (1970). The parcel chosen to represent the air in the updraft was taken from below about 850 mb, assuming the air to be completely mixed.

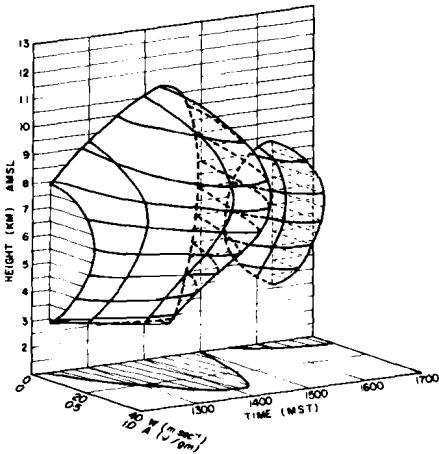


Fig. 7 Same as Fig. 6 except for 29 June 1967.

of golf-ball size was observed. The model is seen to overestimate the storm top by about 2 km but to be consistent with cloud base. The profiles show clearly the effect of the storm in releasing the convective energy. In this case, after storm passage, the instability again began to build up.

6 Conclusions

Ninomiya (1971) has summarized the general conditions that are favorable for the development of severe local storms, as follows: (a) an airstream that is convectively unstable; (b) the availability of moisture in the lower layers within a relatively narrow band; (c) bands of strong winds in the lower and upper levels; (d) some mechanism that can trigger the release of the convective instability. The present analysis supports points (a) and (c). Owing to the limitations of single-station analysis, it is not possible to affirm that the remaining two points of Ninomiya are satisfied in central Alberta. It would be reasonable to suppose that they are, in the absence of contradictory evidence.

The present analysis has shown that the thermodynamic properties of the air, especially those associated with the moisture content, vary considerably over periods in the order of one hour. The radiosonde that is most representative of the storm's ambient air is the one released about two hours ahead of the storm. It is close enough in distance to depict the storm environment and yet far enough away to be unaffected by air which has passed through, and been modified by, the storm.

The one-dimensional, steady-state updraft model, based on slightly modified parcel theory, gives cloud bases and storm tops that are consistent with those observed when the initial parcel is obtained by mixing adiabatically the air from the lowest 300–500 m of the atmosphere. In time sequence the model profiles show the buildup and reduction in convective energy associated with the approach and passage of a storm. When applied to air just behind storms on two occasions the model gave zero positive area and, correspondingly, no vertical velocities.

Acknowledgements

The authors would like to thank the Atmospheric Environment Service for their financial support under contract no. 73494; also Mr. Peter Zwack for very useful discussions on the modification of airflows undergoing differential advection in an upward motion field.

References

- CHISHOLM, A.J., 1970: Alberta hailstorms: a radar study and model. PH.D. thesis. Department of Meteorology, McGill University, May 1970.
- DANIELSON, E.F., R. BLECK and D.A. MORRIS, 1972: Hail growth by stochastic collection in a cumulus model. *J. Atmos. Sci.*, **29**, 135–155.
- HENDERSON, J.H., 1971: The internal structure of a thunderstorm as revealed by θ_w surfaces. *Proc. Seventh Conf on Severe Local Storms*, Kansas City, Oct. 1971, 234–239.
- NINOMIYA, K., 1971: Mesoscale modification of synoptic situations from thunderstorm development as revealed by ATS III and aerological data. *J. Appl. Meteorol.*, **10**, 1103–1121.
- RAGETTE, G., 1973: The low level mesoscale wind field of Alberta hailstorms. To appear in *Mon. Weather Rev.*
- SIMPSON, J., 1971: On cumulus entrainment and one dimensional models. *J. Atmos. Sci.*, **28**, 449–455.
- WARNER, C., J.H. RENICK, M.W. BALSHAW and R.H. DOUGLAS, 1972: Photo and radar studies of Alberta storms. McGill Univ., Stormy Weather Group, Sci. Rep. MW-72, 37 pp.
- WEINSTEIN, A.I., and L.G. DAVIS, 1968: A parameterized model of cumulus convection. Rept. No. 11, NSF Grant GA-777. Department of Meteorology, Pennsylvania State University.
-

The Pseudospectral Approximation Applied to the Shallow Water Equations on a Sphere

Philip E. Merilees¹

*National Center for Atmospheric Research²
Boulder, Colorado*

[Manuscript received 14 October 1972; revised 19 February 1973]

ABSTRACT

An algorithm for the application of the pseudospectral method to the numerical integration of the shallow water equations has been developed and tested on the case of steady-

geostrophic flow over the pole. The results show the method produces errors of less than 1 part in 10^{12} for resolutions as high as $\Delta\lambda = \Delta\phi = \pi/32$.

1 Introduction

There is a particular aspect of numerical weather prediction which has come under severe scrutiny in recent times in conjunction with the GARP program, namely the numerical errors associated with the evaluation of derivatives on a grid. Chouinard and Robert (1972) have shown that with present operational grid lengths, these errors may account for 20% of the rms geopotential height error in a 36-h forecast.

At the same time, since GARP is concerned with global numerical models, there has been considerable concern with the development and evaluation of grid systems on a sphere. These grid systems are usually based on a coordinate system of λ , longitude and ϕ , latitude. Some versions use a constant increment of longitude $\Delta\lambda$ to define the grid, whereas others use a variable $\Delta\lambda$ so that the grid increment is approximately constant in distance. All of these schemes have their particular difficulties as discussed by Williamson and Browning (1972).

Another approach to a global numerical model which circumvents the problems associated with finite differences in a curvilinear coordinate system is the so-called spectral method, which replaces grid-point variables by the coefficients of a set of basis functions, usually spherical harmonics. Models using this approach have been developed by Robert (1968), Machenhauer and Rasmussen (1972) and others. While these models lend themselves beautifully to the global model, they generally require considerably more computer time than corresponding grid-point models. The time-consuming part of the integration of the spectral models is the spectral multiplication.

¹On leave from McGill University, Montreal, Canada.

²The National Center for Atmospheric Research is sponsored by the National Science Foundation.

There is another advantage common to all spectral models which is sometimes forgotten: they have no linear phase error. That is, having expressed a field in terms of a (finite) series of basis functions, we can evaluate the derivative of that field exactly. Since Chouinard and Robert (1972) have shown that the linear phase error accounts for a large part of the difference between integrations at different resolutions, one wonders if it is possible to use the linear property of the spectral method without going to a complete spectral model. Orszag (1972) has discussed a particular method by which this may be done, which he calls the pseudospectral method. The method is to expand a variable at a set of grid points in terms of a set of basis functions; to differentiate the resulting series; and then to evaluate the values of the derivatives at the grid points. No changes are introduced into a particular grid-point model except for the evaluation of derivatives. The particular set of basis functions to be used depends on the particular problem.

This paper will consider the application of the so-called pseudospectral method to the shallow water equations on a sphere and in particular for flows which have an analytical solution.

2 Governing equations

In terms of spherical polar coordinates (λ , longitude; ϕ , latitude) the primitive shallow water equations are:

$$\frac{\partial u}{\partial t} + \mathbf{V} \cdot \nabla u - \left(f + \frac{u}{a} \tan \phi \right) v + \frac{g}{a \cos \phi} \frac{\partial h}{\partial \lambda} = 0, \quad (1)$$

$$\frac{\partial v}{\partial t} + \mathbf{V} \cdot \nabla v + \left(f + \frac{u}{a} \tan \phi \right) u + \frac{g}{a} \frac{\partial h}{\partial \phi} = 0, \quad (2)$$

where

$$\mathbf{V} \cdot \nabla A \equiv \frac{u}{a \cos \phi} \frac{\partial A}{\partial \lambda} + \frac{v}{a} \frac{\partial A}{\partial \phi},$$

u is longitudinal velocity, v is latitudinal velocity, g is acceleration due to gravity, a the radius of the earth, h the height of the free surface, and $f = 2\Omega \sin \phi$ the Coriolis parameter. The equation of continuity is

$$\frac{\partial h}{\partial t} + \nabla \cdot (h\mathbf{V}) = 0 \quad (3)$$

where

$$\nabla \cdot (A\mathbf{V}) = \frac{1}{a \cos \phi} \left[\frac{\partial}{\partial \lambda} (Au) + \frac{\partial}{\partial \phi} (Av \cos \phi) \right].$$

These equations are in the so-called advective form. We may also rewrite these equations in momentum form as

$$\frac{\partial}{\partial t} (hu) + \nabla \cdot (hu\mathbf{V}) - \left(f + \frac{u}{a} \tan \phi \right) hv + \frac{g}{a \cos \phi} \frac{\partial}{\partial \lambda} \frac{h^2}{2} = 0, \quad (4)$$

$$\frac{\partial}{\partial t} (hv) + \nabla \cdot (hv\mathbf{V}) + \left(f + \frac{u}{a} \tan \phi \right) hu + \frac{g}{a} \frac{\partial}{\partial \phi} \frac{h^2}{2} = 0. \quad (5)$$

Equations (1)–(5) are not applicable at the poles since the vector com-

ponents, u , v are not defined. If we wish to use a grid with grid points at the poles, then we can derive appropriate finite-difference expressions for the near pole region by first transforming the equations to some map projection. In this study we shall use another method to circumvent this problem, that is, we shall define a grid which does not have grid points at the poles.

3 Grid-point equations

Let us define a variable

$$\Psi_{nm}^{\tau} = \Psi(\lambda_n, \phi_m, t_{\tau}) \quad (6)$$

where

$$\lambda_n = n\Delta\lambda, \quad \phi_m = m\Delta\phi + \phi_0, \quad t_{\tau} = \tau\Delta t$$

and $\Delta\lambda$ is the longitudinal grid increment, $\Delta\phi$ is the latitudinal grid increment, $\phi_0 = -\pi/2 - \Delta\phi/2$ and Δt is the time step. Then if δ_x denotes a finite-difference operator which is to approximate $\partial/\partial x$, the approximation to equations (1) to (5) can be written as

$$\delta_t u = -\frac{u}{a \cos \phi} \delta_{\lambda} u - \frac{v}{a} \delta_{\phi} u + \left(f + \frac{u}{a} \tan \phi \right) v - \frac{g}{a \cos \phi} \delta_{\lambda} h, \quad (7)$$

$$\delta_t v = -\frac{u}{a \cos \phi} \delta_{\lambda} v - \frac{v}{a} \delta_{\phi} v - \left(f + \frac{u}{a} \tan \phi \right) u - \frac{g}{a} \delta_{\phi} h, \quad (8)$$

$$\delta_t h = -\frac{1}{a \cos \phi} [\delta_{\lambda}(hu) + \delta_{\phi}(hv \cos \phi)], \quad (9)$$

$$\delta_t(hu) = -\frac{1}{a \cos \phi} [\delta_{\lambda}(huu) + \delta_{\phi}(huv \cos \phi)] + \left(f + \frac{u}{a} \tan \phi \right) hv - \frac{g}{a \cos \phi} \delta_{\lambda} \left(\frac{h^2}{2} \right), \quad (10)$$

$$\delta_t(hv) = -\frac{1}{a \cos \phi} [\delta_{\lambda}(huv) + \delta_{\phi}(hvv \cos \phi)] - \left(f + \frac{u}{a} \tan \phi \right) hu - \frac{g}{a} \delta_{\phi} \left(\frac{h^2}{2} \right). \quad (11)$$

In a usual grid-point model, we would then define some appropriate expression for δ_x such as

$$\delta_x = \frac{(\)_{x_{n+1}} - (\)_{x_{n-1}}}{2\Delta x}.$$

The pseudospectral scheme then just involves a different definition of δ_x when x is λ or ϕ .

4 The pseudospectral definition of derivatives

In order to define the pseudospectral derivatives let us consider a variable A_{nm} defined on a grid $n\Delta\lambda, m\Delta\phi + \phi_0$ where $n = 1$ to $2N$, $m = 1$ to M and $N\Delta\lambda = \pi$, $M\Delta\phi = \pi$. We would normally choose ϕ_0 such that the grid point closest to the pole will be $\Delta\phi/2$ away from it. Note that we restrict the number of grid points along a latitude circle to be even, for reasons given below.

The approximation for $\partial/\partial\lambda$ presents no special problem since the variables

are periodic functions of λ and do not involve the pole of the coordinate system. Since A_{nm} is periodic in $n\Delta\lambda$, then we can express A_{nm} as a trigonometric polynomial. We then differentiate this polynomial, and compute the approximation to $\partial A/\partial\lambda$ at the grid points. Therefore we define

$$(\delta_\lambda A)_{nm} \equiv \sum_{k=-(N-1)}^{+(N-1)} ika_m(k) e^{ikn\Delta\lambda} \quad (12)$$

where

$$a_m(k) \equiv \frac{1}{2N} \sum_{n=1}^{2N} A_{nm} e^{-ikn\Delta\lambda} \quad (13)$$

and $i = \sqrt{-1}$. The definition (12) applies for any variable A , whether a scalar or a vector component. In the formulation of a definition of δ_ϕ , however, we must distinguish between a scalar and a vector component.

In the formulation of a pseudospectral approximation to $\partial/\partial\phi$, we might naturally suppose that Legendre functions would form an appropriate set of basis functions. This type of basis is possible, and probably would be the most stable approximation in view of the necessity of dividing by $\cos\phi$ in the dynamical equations. However, there is no known fast transform for Legendre functions, whereas (12) and (13) can be implemented using the fast Fourier transform (Cooley and Tukey, 1965). We therefore define a scheme based on trigonometric functions in latitude, with the expectation that any precision problems which arise because of the division by $\cos\phi$ would be present in a regular grid-point model.

We consider first a scalar quantity. A scalar quantity (such as h , the free surface height) has a continuous derivative at the pole. Therefore we may regard a scalar variable as a continuous periodic function of ϕ as ϕ goes from $-\pi/2$ to $3\pi/2$, simply by changing from a longitude λ to a longitude $\lambda + \pi$ at the poles. Thus if we define an augmented variable B_m such that

$$B_m = A_{nm} \quad \text{for } m = 1 \quad \text{to } M, \quad (14)$$

and

$$B_m = A_{n+N, 2M-m+1} \quad \text{for } m = M+1 \quad \text{to } 2M,$$

then B_m can be expressed as a trigonometric polynomial in $m\Delta\phi$. We may then differentiate the polynomial and evaluate the derivatives with respect to ϕ . We must be careful however to remember that along the longitude $\lambda + \pi$, the derivative of the trigonometric polynomial will in fact approximate $\partial/\partial(-\phi)$. Thus for a scalar variable A we define

$$(\delta_\phi A)_{nm} = \sum_{k=-(M-1)}^{+(M-1)} ikb(k) e^{ikm\Delta\phi} \quad m = 1 \quad \text{to } M \quad (15)$$

$$(\delta_\phi A)_{n+N, 2M-m+1} = - \sum_{k=-(M-1)}^{+(M-1)} ikb(k) e^{ikm\Delta\phi} \quad m = M+1 \quad \text{to } 2M \quad (16)$$

where

$$b(k) = \frac{1}{2M} \sum_{m=1}^{2M} B_m e^{-ikm\Delta\phi}, \quad (17)$$

and B_m is as defined by (14). A vector component is not in general continuous at the poles. For example, if we have a north wind on one side of the pole, we will have a south wind at the other side. However, the actual wind is continuous across the pole. If however we construct a function of ϕ from $\phi = -\pi/2$ to $3\pi/2$ where we change the sign of the variable when we cross the pole, we can regard this function as a continuous periodic function of ϕ and apply the pseudospectral algorithm. However in this case the derivative with respect to ϕ along longitude $\lambda + \pi$ will be given directly (without change of sign) since the two changes in sign will cancel.

Therefore the derivative of a vector component A is approximated by

$$(\delta_\phi A)_{nm} = \sum_{k=-(M-1)}^{+(M-1)} ikb(k) e^{ikm\Delta\phi}, \quad m = 1 \text{ to } M \quad (18)$$

$$(\delta_\phi A)_{n+N, 2M-m+1} = \sum_{k=-(M-1)}^{+(M-1)} ikb(k) e^{ikm\Delta\phi}, \quad m = M+1 \text{ to } 2M \quad (19)$$

where

$$b(k) = \frac{1}{2M} \sum_{m=1}^{2M} B_m e^{-ikm\Delta\phi}, \quad (20)$$

and B_m is defined as follows;

$$\begin{aligned} B_m &= A_{nm} && \text{for } m = 1 \text{ to } M, \\ B_m &= -A_{n+N, 2M-m+1} && \text{for } m = M+1 \text{ to } 2M. \end{aligned} \quad (21)$$

We note that since we choose an even number of grid points around a latitude circle there is always a grid line $\lambda + \pi$ corresponding to grid line λ . It is possible to modify the algorithms for an odd number of points, but since we plan to calculate the transforms using the fast Fourier transform which is most efficient when the number of points is a power of 2, this does not seem to be a serious restriction.

5 Test of the algorithms

As a first test of the pseudospectral method of evaluating derivatives we consider their application to the shallow water equations using initial conditions which are a steady-state analytic solution. The solution corresponds to zonal geostrophic flow. We do however rotate the coordinate system and discrete grid through an angle α so that the finite-difference expressions are not satisfied trivially. Here we follow Williamson and Browning (1972) and define as initial conditions

$$\left. \begin{aligned} u &= u_0(\cos \phi \cos \alpha - \cos \lambda \sin \phi \sin \alpha) \\ v &= u_0 \sin \lambda \sin \alpha \\ h &= h_0 - h^*(\cos \lambda \cos \phi \sin \alpha + \sin \phi \cos \alpha)^2 \\ f &= 2\Omega(\cos \lambda \cos \phi \sin \alpha + \sin \phi \cos \alpha) \end{aligned} \right\} \quad (22)$$

where

$$h^* = \frac{1}{g} (a\Omega u_0 + \frac{1}{2}u_0^2).$$

We note that the highest wave number which appears in (22) is 2 (e.g., $\cos^2 \lambda$

$= \frac{1}{2} (1 + \cos 2\lambda)$). Therefore we should expect the pseudospectral method to give very good results if $N > 2$ when the equations are in the advective form and if $N > 4$ when the equations are in the flux form. For the test then, we choose $N = 8$, $M = 8$ which has the further advantage that N is a power of 2 so that the fast Fourier transform used to evaluate the algorithms is efficient. We take two cases of α to be representative, namely $\alpha = \pi/4$ and $\pi/2$, and use the following values for the constants in (22),

$$u_0 = 5 \text{ m s}^{-1} \quad gh_0 = 2.94 \times 10^4 \text{ m}^2 \text{ s}^{-2} \quad \Omega = 7.292 \times 10^{-5} \text{ s}^{-1}$$

$$a = 6.37122 \times 10^6 \text{ m} \quad g = 9.80616 \text{ m s}^{-2}.$$

We further note in Equations (7) to (11) that for the purposes of approximating the derivatives with respect to ϕ we treat u , v , $huv \cos \phi$ and $hvv \cos \phi$ as vector components since their signs will depend on the definition of the coordinate system whereas the sign of $hv \cos \phi$ does not.

6 Results

Ideally, since the initial conditions lead analytically to a steady-state flow, we should find that the right-hand sides of Equations (7) to (11) are identically zero. As a measure of the accuracy of the pseudospectral scheme we compute the ratio of the rms value of the right-hand side for each of (7) to (11) compared to the rms value of the sum of the absolute values of the right-hand sides of (7) to (11). We also compare the largest residual of the right-hand side to the rms value of the sum of the absolute values of the right-hand side. In Table 1 we present these ratios for the advective form ($\alpha = \pi/2$) and for the flux form ($\alpha = \pi/4$) of the equations for a grid resolution of $\Delta\lambda = \Delta\phi = \pi/8$.

TABLE 1. The ratio of the indicated term to the sum of the absolute values of the components of that term. Column labelled RMS is the ratio of rms values, that labelled MAX is the ratio of the maximum value of the indicated term to the rms value of the sum of absolute values. The grid size here is $\Delta\lambda = \Delta\phi = \pi/8$.

Term	$\alpha = \pi/4$		$\alpha = \pi/2$	
	RMS	MAX	RMS	MAX
$\frac{\partial u}{\partial t}$	2.30×10^{-13}	6.23×10^{-13}	1.81×10^{-13}	6.42×10^{-13}
$\frac{\partial v}{\partial t}$	6.93×10^{-14}	1.96×10^{-13}	1.17×10^{-13}	3.33×10^{-13}
$\frac{\partial h}{\partial t}$	3.62×10^{-14}	1.38×10^{-14}	3.45×10^{-14}	2.15×10^{-13}
$\frac{\partial hu}{\partial t}$	2.89×10^{-13}	6.22×10^{-13}	1.78×10^{-13}	8.56×10^{-13}
$\frac{\partial hv}{\partial t}$	8.78×10^{-14}	2.65×10^{-13}	1.15×10^{-13}	3.42×10^{-13}

In order to interpret Tables 1 and 2 more clearly we note that the order of magnitude of the individual terms on the right-hand sides of the dynamical

TABLE 2. Same as Table 1 except $\Delta\lambda = \Delta\phi = \pi/32$.

Term	$\alpha = \pi/4$		$\alpha = \pi/2$	
	RMS	MAX	RMS	MAX
$\frac{\partial u}{\partial t}$	2.44×10^{-12}	1.79×10^{-11}	1.34×10^{-12}	7.01×10^{-12}
$\frac{\partial v}{\partial t}$	3.37×10^{-13}	1.82×10^{-12}	4.77×10^{-13}	2.12×10^{-12}
$\frac{\partial h}{\partial t}$	1.71×10^{-13}	1.53×10^{-12}	1.64×10^{-13}	1.67×10^{-12}
$\frac{\partial hu}{\partial t}$	1.82×10^{-12}	1.65×10^{-11}	2.31×10^{-12}	1.79×10^{-11}
$\frac{\partial hv}{\partial t}$	4.17×10^{-13}	1.56×10^{-12}	4.90×10^{-13}	1.70×10^{-12}

equations is fu_0 for the advective form and fh_0u_0 for the flux form. Thus the order of magnitude of $\partial hu/\partial t$ in the case $\alpha = \pi/4$ with $\Delta\lambda = \Delta\phi = \pi/8$ in dimensional units is $10^{-12} \text{ m}^2 \text{ s}^{-2}$ whereas Williamson and Browning found values of $\partial hu/\partial t$ of the order of $10^{-1} \text{ m}^2 \text{ s}^{-2}$ using a second-order finite-difference scheme with $\Delta\lambda = \Delta\phi = \pi/36$.

The calculation indicates the flow is stationary to about 13 decimal places. Since the computations were performed with 15-decimal precision, we have therefore lost a couple of decimals precision in the transform calculations.

As discussed previously we might expect to lose some precision as the resolution is increased because of the necessity of dividing by $\cos \phi$ when ϕ is close to $\pm\pi/2$. In order to illustrate this effect the computation was performed with a resolution of $\Delta\lambda = \Delta\phi = \pi/32$ and the results are presented in Table 2. Here we note that we have lost another decimal place in the rms accuracy and about two decimal places in the maximum error. By inspecting the grid-point values of these quantities we can verify that the maximum error occurs at grid points next to the poles. In fact for grid points away from the pole there is very little difference between the two resolutions.

7 Final remarks

The algorithm we have developed here produces remarkably accurate results for the particular initial conditions we have chosen as a test. It is not clear however, if the same accuracy will be obtained for flow fields which are more realistic. Further, there are questions about the relative speed of this algorithm versus a standard finite-difference technique. Therefore, we should subject the algorithm to further tests and comparisons with standard techniques using realistic initial conditions in order to further evaluate its worth.

Finally we note that the algorithm has another advantage, in that a trivial modification will provide smoothing of the derivatives as desired.

Acknowledgements

The author is indebted to S. Orszag who pointed out the pseudospectral method and to D. Williamson for many helpful discussions.

References

- CHOUINARD, C., and A. J. ROBERT, 1972: Truncation errors in a filtered barotropic model. *Proc. 9th Stanstead Seminar*. Publ. in Meteorology No. 103, McGill Univ., 136 pp.
- COOLEY, J. W., and J. W. TUKEY, 1965: An algorithm for the machine computation of complex Fourier series. *Math. Comp.*, **19**, 297-301.
- MACHENHAUER, B., and E. RASMUSSEN, 1972: On the integration of the spectral hydrodynamical equations by a transform method. Rep. No. 3, Inst. Teoretisk Meteorologi, Københavns Univ., 44 pp.
- ORSZAG, S. A., 1972: Comparison of pseudo-spectral and spectral approximations. *Studies Appl. Math.*, **51**, 253-259.
- ROBERT, A. J., 1968: Integration of a special barotropic model from global 500-mb charts. *Mon. Weather Rev.*, **96**, 83-85.
- WILLIAMSON, D., and G. L. BROWNING, 1972: Comparison of grids and difference approximations for numerical weather prediction over a sphere. NCAR/LAS Manuscript 2120-72-1, 34 pp.

BOOK REVIEWS

MÉTÉOROLOGIE ET AÉRODYNAMIQUE DE LA POLLUTION ATMOSPHÉRIQUE. Par J. Lacaze. Editions Jacques Fréal, 114 rue de Grenelle, Paris, 1972, 80 pp.

Ce petit livre sans prétention a le mérite de ramasser en quelques pages les équations qui régissent la diffusion des polluants dans l'atmosphère et de faire le point sur les résultats de la recherche en ce domaine. L'auteur se veut pratique, non-théoricien : il néglige donc délibérément les démonstrations théoriques et il ne fait que présenter les résultats acquis. Il va même, de propos délibéré, jusqu'à supprimer toute bibliographie, ce qui me semble aller trop loin : nul doute que plusieurs lecteurs auraient aimé retrouver facilement la référence des auteurs cités. Ils auraient alors pu compléter les explications si souvent maigres et un peu courtes de l'Auteur. A cause de cela, le livre me semble s'adresser moins "aux industriels, urbanistes et hygiénistes" comme le prétend l'auteur ou l'éditeur dans la page frontispice, mais plutôt à des météorologistes déjà avertis. L'utilisation des équations et formules de ce recueil sans plus de critique par de non-spécialistes m'apparaîtrait très dangereuse et téméraire.

L'auteur offre des réflexions assez personnelles sur le rôle trop souvent négligé de l'humidité dans la stabilité atmosphérique, sur le rôle de la rotation de la terre dans l'établissement de la couche limite. Il note aussi à bon droit que "la seule existence d'une surface d'inversion n'est pas le critère absolu d'accumulation des polluants et qu'un vent moyen, faible et persistant de direction peu variable avec z, est la condition réellement indispensable, en plus de la stabilité dans les basses couches, pour que les pollutions proches soient fortes" (pages 27 et 28). Les figures relèvent davantage de l'artisanat que d'un graphisme de ton professionnel, mais elles sont claires et suffisamment grandes. Quant aux équations, elles ne traînent guère avec elles beaucoup d'explication et il est difficile de s'imaginer comment "les industriels, les urbanistes et hygiénistes" peuvent s'y démêler. Pour cette raison encore, le livre me semble s'adresser davantage aux spécialistes comme un recueil et une mise au point rapide du savoir-faire en ce domaine.

Conrad East
Centre de recherches écologiques
Université du Québec à Montréal

Book Reviews continued on page 34

A Case Study of Mixing-Height Variations in the Toronto Area

B. Padmanabhamurty¹ and R.E. Munn
*Atmospheric Environment Service,
Toronto, Canada*

[Manuscript received 20 March 1973]

ABSTRACT

The variation of mixing height in the Toronto area is investigated using data from 3 rawinsonde stations which made special observations at 2-hourly intervals during 9 days in December 1970. The afternoon maximum mixing heights were estimated in two ways: (a) from the sequence of rawinsonde flights; (b) from the 1200 GMT sounding and the afternoon maximum surface temperature (the

standard method applied to the synoptic twice-a-day network of rawinsonde stations across North America). A comparison of the two estimates reveals considerable scatter, presumably due to mesometeorological variations and advection effects. Also included in this note is a description of a case of doming of the early morning mixed layer over downtown Toronto.

1 Introduction

During 9 days in December 1970, an interesting feasibility study for the IFYGL was undertaken in the Toronto area: rawinsonde flights were made at 2-hourly intervals at Scarborough, Front Street and at a location near the Oakville-Burlington town line. (See Fig. 1.) (Ferguson and Schaefer, 1971.)

A network with such a space and time density is rarely available near and within a large urban area. It therefore seemed desirable to re-examine the observations from the point of view of the urban meteorologist. Admittedly, the data sample was small, and the subset of days was not selected to coincide with air pollution episodes: in fact, a succession of frontal systems crossed the Toronto area during the period. About the most that can be said is that the data set was randomly selected from the point of view of an urban boundary-layer investigation.

2 Method of analysis

Sixty-one simultaneous flights were scheduled, but there were a few missing observations due to strong winds, etc. For the present study, the baroswitch ascent data were plotted up to the 800-mb level only, and the mixing height at each observational hour was determined by the conventional method of fol-

¹NRC Post-Doctoral Fellow, present address: Meteorological Office, Poona 5, India.

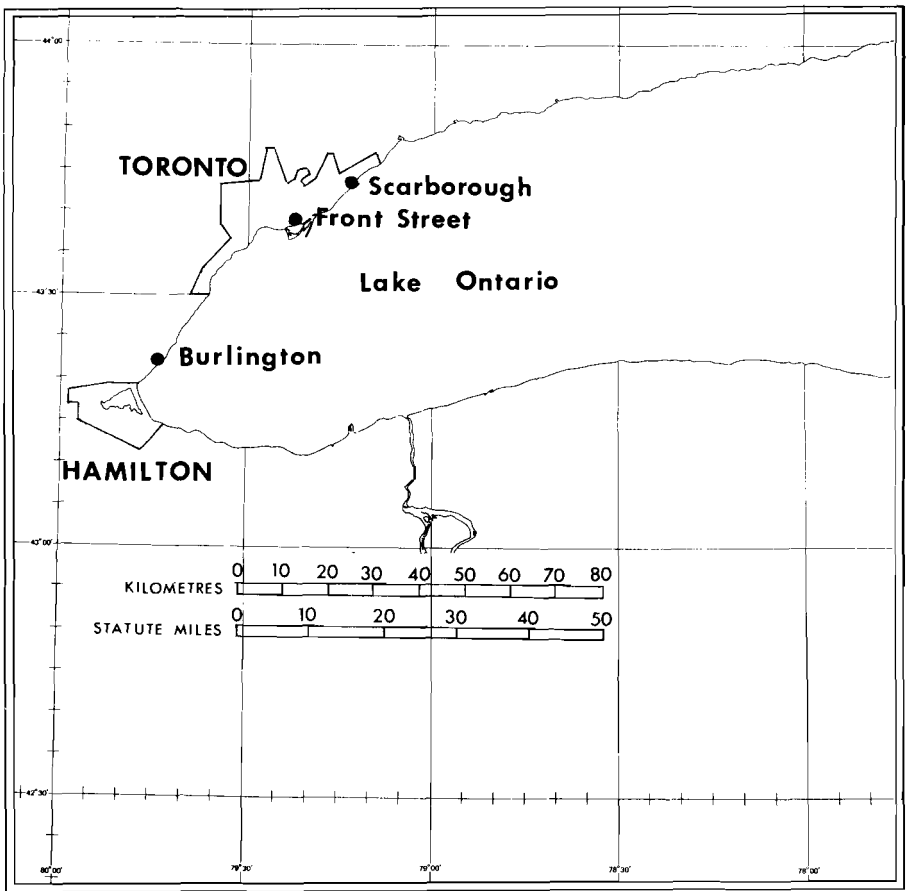


Fig. 1 Map showing location of observing sites.

lowing a dry adiabat at the surface temperature up to its intersection with the ascent curve. The largest afternoon value was assumed to be the maximum.

To obtain a second estimate of the maximum afternoon mixing height, the 1200 GMT ascent curve was used together with the maximum temperatures reported at the nearest climatological stations: Scarborough, Toronto Bloor Street (representative of Front Street) and Burlington. This is the method that is widely used to derive synoptic-scale mixing-height climatologies from standard rawinsonde stations that take only two flights a day (Holzworth, 1969).

3 Results and discussion

a Time Sequence of Mixing Heights

Fig. 2 shows the time sequence of mixing heights at the three stations. There appears to be no systematic variation in mixing heights in time or space but one can at least generalize that values are usually higher in the afternoon than at night. The variability is no doubt due to the succession of pressure systems

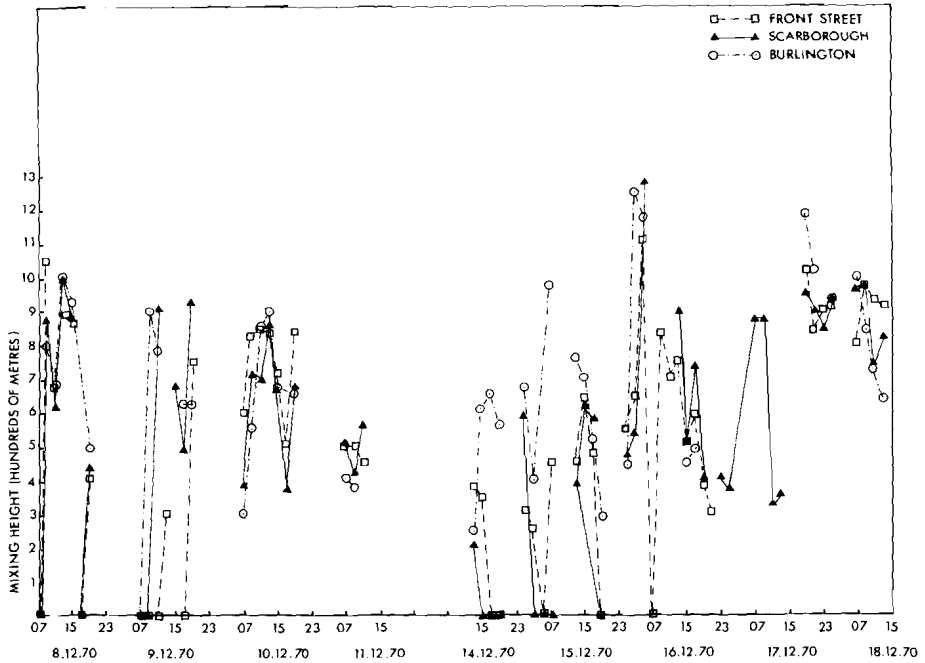


Fig. 2 Time sequence (EST) of the surface mixing heights at the three observing stations.

that crossed the region during this period. On the evening of December 17, for example, strong gusty east winds developed.

b Actual Versus Predicted Maximum Afternoon Mixing Heights

Fig. 3 is a plot of actual (i.e., that obtained from a succession of flights) vs. predicted (i.e., that obtained from a 1200 GMT sounding) maximum afternoon mixing heights for all available cases. The scatter is large, undoubtedly due in part to the fact that the data sample is small and that the synoptic weather patterns were not "steady state". Advection of colder or warmer air between 1200 GMT and the time of the day-time maximum temperature no doubt contributes to the scatter. The results do indicate, however, that for a shoreline location in or near a large city, the estimate of maximum afternoon mixing height obtained from the 1200 GMT ascent at the nearest rawinsonde station may be considerably in error.

c Effect of the Urban Heat Island on Mixing Heights

On December 10, 1970, winds at all three locations remained in the wind sector NW-N-NE. Supplementary observations from two towers, one at a lakeshore site in west Toronto, the other at a rural site northwest of Toronto (the Meteorological Research Station), indicated that: (1) the wind at 46–91 m averaged about 6.7 m s^{-1} , slackening to about 2 m s^{-1} in the evening; (2) the lapse rate in the lowest 46–91 m remained near the adiabatic in the early morning, becoming slightly superadiabatic during the day.

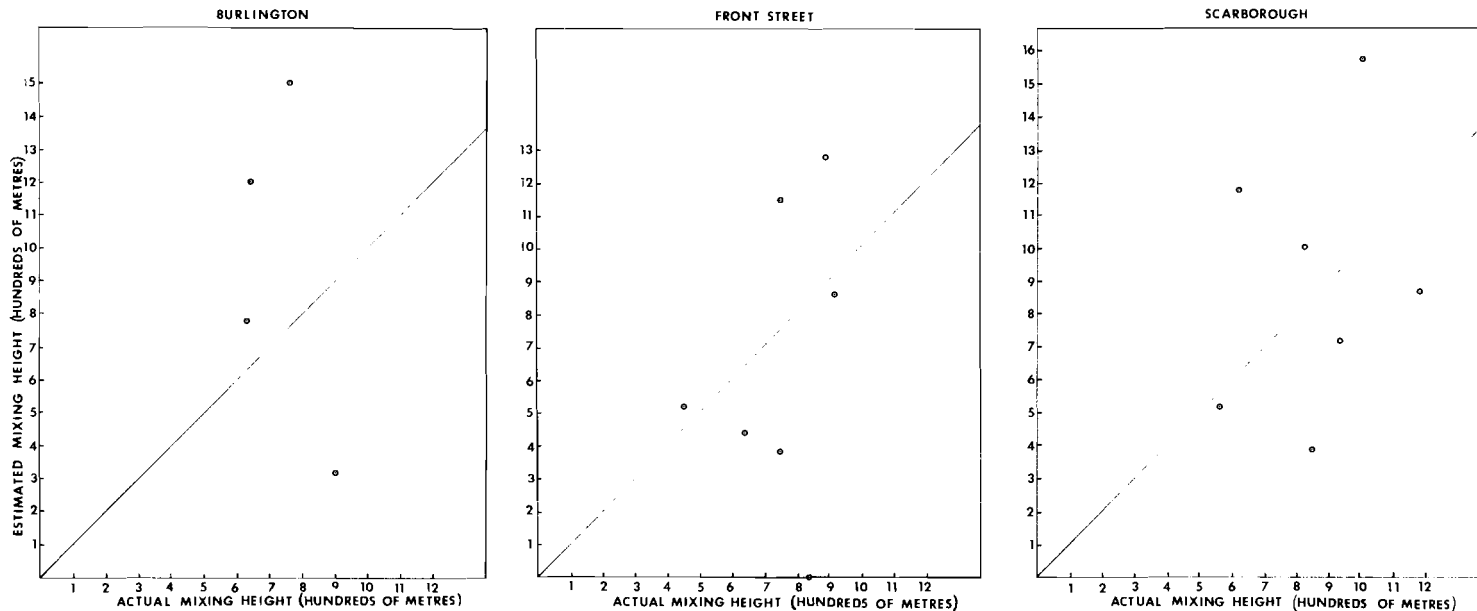


Fig. 3 Scatter diagrams of actual (i.e., that obtained from a succession of flights) vs. predicted (i.e., that obtained from a 1200 GMT sounding) maximum afternoon mixing heights, for each of the three stations.

With northerly winds, the Front Street rawinsonde site is close to the centre of the Toronto heat island in the built-up downtown core. Scarborough with these winds may be classified as suburban, and Burlington as rural. Table 1

TABLE 1 Mixing heights (m) in the Toronto area on December 10, 1970.

Time (EST)	Scarborough	Front St.	Burlington
0700	390	600	310
0900	710	830	560
1100	700	860	870
1300	850	840	900
1500	660	720	675
1700	370	505	—
1900	680	840	660

shows the mixing heights for December 10, and there is evidence for a “doming” of the surface layer over the urban core both in the morning and again in the evening. This is in agreement with the observations over St. Louis described by Spangler (1972). In the early afternoon (1300 EST), the mixing heights are about the same at all three stations.

4 Conclusion

The height of the surface mixed layer is of considerable importance in the prediction of pollution potential and of pollution concentrations. Although the synoptic-scale network of rawinsonde stations may provide useful mixing-height climatologies, they may not be accurate predictors (in the North American time zones) of maximum afternoon mixing heights on a day-to-day basis. In addition, they may not be representative of neighbouring urban, coastal or valley locations.

For operational prediction systems, therefore, there is a need for supplementary observations using either slow-rise balloons or remote-sensing techniques. In this connection, it should be noted that continuous measurements from suitably-located tall towers yield useful information on the mean wind within the surface mixed layer (another important predictor of air quality) but rarely extend sufficiently far upward to penetrate through the top of the surface layer.

References

- FERGUSON, H.L., and D.G. SCHAEFER, 1971: Feasibility studies for the IFYGL atmospheric water balance project. *Proc. 14th Conf. Great Lakes Res.*, 438–453.
- HOLZWORTH, G.C., 1969: Large-scale weather influences on community air pollution potential in the United States. *J. Air Pollut. Cont. Assoc.*, **19**, 248–254.
- SPANGLER, T.C., 1972: Dynamically induced mesoscale variations of the urban mixing layer depth. Rept. No. AR104, Dept. of Atmos. Res., College of Eng., Univ. of Wyoming, Laramie, U.S.A., 30 pp.

A Note on Waves, Wavegroups, and Local Influence

James H.S. Bradley

Physics Department, Drexel University, Philadelphia, Pennsylvania

[Manuscript received 31 July 1972]

ABSTRACT

The observed meridional motions of atmospheric systems or wavegroups are shown to be related to the shape-preserving (normal mode, eigenfunction) waves discussed in linearized perturbation theory through the concepts of group velocity, dispersion and interference pattern. Although all phase velocities are east-west, the group velocity vector can lie in any

direction. Phase velocities with a meridional component can occur if the Coriolis parameter is replaced by a linear function of latitude only because the proper periodic boundary condition cannot then be imposed. Orographic effects make the phase velocity non-existent in a hydrostatic atmosphere, but the concept of group velocity remains valid.

The novice meteorologist is often shown a weather map bearing various systems described as waves: frontal waves, short waves, long waves, troughs and ridges. These systems change in size, shape, thermal structure and latitude as well as longitude and intensity. On the other hand most textbooks of meteorological dynamics introduce him to linearized perturbation theory which describes waves incapable of changing in size, shape, structure or latitude. The usual theories of baroclinic stability allow changes of amplitude, but the waves observed on a map do not agree with the other theoretical postulates. The impression is therefore liable to be left that the assumptions made in the theory have somehow made its relation to the atmosphere rather remote, so that realism could be achieved only by the non-linear equations or at least through the removal of the common assumptions of steady east-west flows in the basic state on a so-called beta plane. The author does not wish to give anybody the impression that the assumptions made in some undergraduate texts offer mathematical convenience or physical advantage; yet their consequences are not destructive for the reasons which some people seem to believe.

Examination of the Rossby-Haurwitz theory of non-divergent motions in a barotropically stratified fluid in solid rotation about the earth's axis reveals that once again the textbook treatments describe only east-west motions of waves incapable of changing in size or shape; the trouble is therefore apparently not due to the textbook forms of the beta plane assumption. The pursuit of material not available in textbooks, such as the replacement of the Coriolis parameter sinusoid by other functions which yield elementary solutions or cases with meridional shears of the zonal wind, leads to the same conclusion. One can, for instance, derive the coefficients of linear functions of latitude to

replace the Coriolis parameter which yield solutions optimal in a wide variety of different senses; the beta plane is merely the non-optimal prescription of the linear function as a tangent to the Coriolis sinusoid.

When one replaces the Coriolis parameter sinusoid by some linear or other function it may be possible to imagine meridional motions in a purely advective sense, the phase velocity remaining strictly east-west relative to the atmosphere. Unfortunately this illustrates only the radical influence which can be exerted by the destruction of the natural boundary condition of periodicity around the earth. Meridional motion of shape-preserving waves is not possible in rotating spherical coordinates with periodic boundary conditions.

Unfortunately the dichotomy is fundamental, being due to the anisotropy caused by the absolute rotation of the atmosphere about an axis which is close to the earth's axis. Adventures into all kinds of shears and stratifications in steady basic states lead into some difficulties with non-separable or non-Sturm-Liouville equations which can be overcome by a wide variety of methods: Galerkin, moment, Frobenius series, modern eigensystem algorithm (Wilkinson, 1965; Fadeev and Fadeeva, 1960) and others; yet within the framework of any steady basic state the shape-preserving normal modes (eigenfunctions) remain incapable of change in size, shape, structure or latitude. This is true even of the most ingenious and complicated solutions given in the excellent work of Professor M.S. Longuet-Higgins, F.R.S., (1964, 1965), who is now at Cambridge.

The methods of examining the convergence of perturbation approximations which are routinely used and demanded in atomic, molecular and nuclear physics permit the analysis of many basic states which are otherwise intractable, and deserve to be routinely taught in meteorology. A more widespread application of such methods would have made the fundamental nature of the dichotomy well known.

Are we then to fall back on unsteady basic states and non-linear effects? Now it is true that unsteady basic states can lead to normal modes capable of changing in size and shape, in those cases when the time dependence is non-separable. Yet the life of a typical mid-latitude cyclone at around 3 to 5 days is considerably shorter than the index cycle at around 15 days, no matter whose definition of the circulation index one prefers; indeed the circulation index for solid rotation by pressure levels p , at time t

$$\alpha(p, t) = \frac{1}{s} \int (u/a \cos \phi) ds \quad (1)$$

(where u is the eastward velocity, a the radius of the earth, ϕ latitude and s the entire surface of the earth) has a predominantly annual cycle. Observational studies (Bradley and Wiin-Nielsen, 1968; Meshcherskaya *et al.*, 1970) indicate that changes in the shape of the eigenfunctions of the real atmosphere are very small and very gradual. One cannot fall back on the non-linear hypothesis that no such shape preserving waves exist.

The important concepts in understanding changes of size, shape, thermal

structure and latitude are group velocity, dispersion and interference pattern; Longuet-Higgins (1964) gives some elementary treatments, and also discusses the orographic reflexion of rotational waves. For instance, within the framework of non-divergent perturbations in a barotropically stratified atmosphere with a lid, at rest relative to the coordinate system, the replacement of the Coriolis parameter by any straight line of slope β leads (under appropriate boundary conditions) to shape-preserving waves (normal modes, eigenfunctions)

$$\exp [i(kx + ly - \sigma t)],$$

where x is the easterly coordinate, y the northerly coordinate, t time, and σ frequency, and where k and l are wave numbers obeying

$$(k, l) = (m \cos \delta, m \sin \delta) \quad (2)$$

where δ is the angle between the x axis and a line perpendicular to the wave crests, and m is the total wave number.

The phase velocity is

$$c = \sigma/k = -\beta/m^2 \quad (3)$$

towards the west relative to the bulk flow, but the group velocity has components

$$\begin{aligned} \partial\sigma/\partial k &= (\beta \cos 2\delta)/m^2 \\ \partial\sigma/\partial l &= (\beta \sin 2\delta)/m^2 \end{aligned} \quad (4)$$

The group velocity represents the velocity vector of the interference patterns which are meteorological systems; changes of size, shape, structure, latitude and intensity represent either dispersion or changes in amplitude of the constituent waves. Of course the normal modes of the real atmosphere are not sinusoids, but approximately surface harmonics (Eliassen and Machenhauer, 1969; and earlier papers; also many papers by Deland and his pupils) or Hough functions (Hough, 1898) or empirical orthogonal functions (Bradley and Wiin-Nielsen, 1968). The real atmosphere has 16 to 18 longitudinal modes, 4 to 6 meridional modes and 3 to 5 vertical modes of appreciable intensity. Their shapes are very stable, which is another indication that unsteadiness of the basic state is a minor effect in the real atmosphere. The concept of group velocity can be extended to the interference patterns of the non-sinusoidal waves which arise in all mathematically satisfactory theories.

The author has constructed some simple demonstrations to illustrate group velocities in undergraduate general meteorology classes open to all scientists and engineers. The simplest consists of parallel bands (2.54-cm wide) ruled on transparencies; superposition of two such transparencies at a small angle yields an interference pattern of Moiré fringes in which a phase velocity normal to the wave crests yields a group velocity parallel to the crests. Slightly more complicated demonstrations have been made by superposing transparencies with rulings of different spacings, and by superposing transparencies marked only with the positive and negative regions of surface harmonics in any convenient hemispheric map projection. Nowadays lamps, ornaments, and mobiles artistically exploiting Moiré effects are widely sold.

Unfortunately the concept of group velocity appears to be used in only two meteorological textbooks (Petterssen, 1956; Laikhtman *et al.*, 1967), and then only in the simplest $\exp[i(kx - \sigma t)]$ representation of the Rossby barotropic beta plane theory; consequently the reader is left with the impression that the phase and group velocity vectors are necessarily east-west. The concept of group velocity is certainly implicit but apparently nowhere explicit in the modern literature on observed planetary wave motions.

Further theoretical complications arise from the imposition of the hydrostatic assumption, which by rendering infinite the speed of vertical propagation of disturbances of pressure excludes vertical propagation. The imposition of realistic orographic lower boundary conditions is liable to make the east-west dependence non-sinusoidal and possibly non-separable; in this case the phase velocity does not exist in a hydrostatic atmosphere but the concepts of group velocity and interference pattern remain valid. Fortunately the author's observations of geopotentials and clouds indicate that the east-west eigenfunctions are sinusoids within the statistical sampling fluctuations.

Those waves which remain of finite amplitude in the real atmosphere must have frequencies σ which are pure real when averaged over a long period of time, usually a few days. Sound and gravity waves and the higher rotational modes appear to decay at all times. Just as in the case of an electrical oscillator, the amplitude of the meteorological waves is presumably governed by the fact that their dissipation increases and their power supply weakens with increasing amplitude in such a manner that

$$\partial \text{imag}(\sigma) / \partial \text{amplitude} = 0 \quad (5)$$

on the average, and the second derivative is positive (small waves grow, large waves decay).

Any forecast model uses Galerkin or finite-element methods (finite-difference methods being the least economical and least powerful case of the finite element method, which is a Galerkin method based on spline polynomials with piecewise continuous derivatives) to reduce the differential operators and eigenfunctions of the real atmosphere to some matrix eigensystem having a finite number of shape preserving waves and corresponding frequencies. It is more important that such matrices reproduce the group velocity than the phase velocity in the low frequency region of the meteorological waves, which are the rotational solutions of the linearized versions of the dynamic equations representing all possible wave motions in real dry atmospheres, which were derived by Laplace (1799).

The link between the shape-preserving-wave view of nature and the local influence view which comes naturally to a forecaster (especially when his charts cover only a fraction of one hemisphere) may be made through the Green's function, though usually only conceptually because the Green's functions of physically interesting cases are prohibitive to calculate explicitly. A good treatment of Green's function methods is available in Kibel (1957).

The standards of physics and mathematics demanded of meteorologists, at Drexel, and at a few other schools make it easy to teach group velocities and

the Laplace tidal equations to undergraduates, and to teach all the relevant work in first graduate courses. At Drexel the Longuet-Higgins papers are routinely used for this purpose, in introductory graduate courses based on Eckart's *Hydrodynamics of Oceans and Atmospheres* (Pergamon, 1960).

References

- BRADLEY, J.H.S., and A.C. WIIN-NIELSEN, 1968: On the transient part of the atmospheric planetary waves. *Tellus*, **20**, 533-544.
- ELIASSEN, E., and B. MACHENHAUER, 1969: On the observed large-scale atmospheric wave motions. *Tellus*, **21**, 149-166.
- FADEEV, V.N., and D.K. FADEEVA, 1960: *Chislennye Metodi Linearnoi Algebr. Gostekhizdat*, 621 pp. Translated (1963) as: *Computational Methods of Linear Algebra*. Freeman, San Francisco.
- HOUGH, S.S., 1898: On the application of harmonic analysis to the dynamical theory of the tides. Part II. On the general integration of Laplace's dynamical equations. *Phil. Trans. Roy. Soc.* **A191**, 139-185.
- KIBEL, I.A. 1957: *Hydrodynamic Methods of Short Period Weather Forecasting*. Translation 1963, Pergamon Press, 383 pp.
- LAIKHTMAN, D.L., L.S. GANDIN and others, 1967: *Problems in Dynamic Meteorology*. Translation 1970, WMO publication No. 261. TP.146, 245 pp.
- LAPLACE, P.S., 1799: *Mécanique Céleste*. Part 2, Vol. 4, Paris.
- LONGUET-HIGGINS, M.S., 1964: Planetary waves on a rotating sphere. *Proc. Roy. Soc.* **A279**, 446-473.
- , 1965: Planetary waves on a rotating sphere, Part 2. *Proc. Roy. Soc.*, **A284**, 40-68.
- MESHCHERSKAYA, A.V., L.V. RUKHOVETS, M.I. YUDIN and N.I. YAKOVLEVA, 1970: *Estestvennii Sostavlyayushchie Meteorologicheskikh Polei. Gidrometeoizdat*, 199 pp.
- PETTERSSSEN, S., 1956: *Weather Analysis and Forecasting*, Vol. 1. McGraw-Hill, 428 pp.
- WILKINSON, J.H., 1965: *The Algebraic Eigenvalue Problem*. Oxford University Press, 662 pp.

NOTES FROM COUNCIL

The following were accepted as members by Council:

December 18, 1972

<i>Member</i>	George Isaac Oscar Koren	Michael Rejean Lafrance Joseph Edward Shaykewich
<i>Student Member</i>	Robert N. Goethe	Michel-Germain Perrier

January 31, 1973

<i>Member</i>	Han-Ru Cho Arthur B. Cooper Edwin A. S. Galbraith Leonard A. Heapy P. André Lachapelle	Lloyd T. Millar William Louis Ranahan Joseph L. Rood William David Wyllie
<i>Student Member</i>	Joan V. Jensen	Thomas Michael Morrow

February 27, 1973

<i>Member</i>	John Edward Moroz	Stanley Francis Woronko
<i>Student Member</i>	Myron Morris Oleskiw	

A Mirage at Regina

John R. Hendricks

Atmospheric Environment Service, Regina

[Manuscript received 12 December 1972]

ABSTRACT

The Dirt Hills, located roughly forty miles to the southwest of the Regina Weather Office, at Regina, Saskatchewan, were clearly visible on the horizon in the early morning of the 29th

day of August 1972 from the Regina Weather Office. This mirage was documented and a picture of it was taken.

1 Introduction

The 28th day of August 1972 was a hot day at Regina. It began as a warm day when the early morning temperatures showed a minimum of 61°F. This was a new high minimum temperature record for the date.

The southwesterly flow of dry air blowing across southern Saskatchewan meant that the local people would experience a blistering afternoon. And, so they did. The temperature reached 94 degrees and established a new temperature record for the date. Moose Jaw, some forty miles to the west, also set a new record high temperature for the 28th day of August with a reading of 95 degrees.

With this as background, and knowing that mirages are frequently seen in the early morning at Regina during spells of hot weather, camera, lenses and sundry equipment were taken to the Regina Weather Office in anticipation of an early morning mirage, likely to occur as a climax to the midnight shift.

2 The mirage

When the sun rose at 6:07 CST on the 29th day of August 1972, a mirage was visible on all horizons. Those features which were normally situated beyond the horizon seemed to be tilted upwards into view. Things which were normally expected to be far away appeared to be much closer.

Many slides were taken between 6:15 and 6:30 CST from the rooftop adjacent to the Regina Weather Office. The best of all the pictures is shown in Fig. 1. The mirage gradually disappeared between 8 and 9 a.m.

The normal scene to the southwest of Regina is flat farm land (Fig. 2). The Dirt Hills and Cactus Hills, situated near Claybank, Saskatchewan, roughly forty miles to the southwest of Regina, are normally out of view. These hills are shown clearly in Fig. 1.



Fig. 1 This view was taken from the roof adjacent to the Regina Weather Office on the day of the mirage using a 300-mm lens and looking towards the southwest. The radar tower in the picture is at about 210° from true north at this vantage point.



Fig. 2 This view is taken from the same spot as for the view in Fig. 1, but on the day after the mirage using a 55-mm lens with a $3\times$ converter.

3 Meteorological conditions

At 6:00 a.m., or 1200 GMT, the usual pilot balloon was launched at the Regina Weather Office and showed the following wind profile aloft:

Wind level (ft)	Direction(°)	Speed (kt)
surface	120	12
3000	210	38
4000	250	38
5000	250	38
6000	235	38
7000	250	24
8000	250	20
9000	240	20

Saskatchewan does not have a radiosonde station. The vertical temperature distribution over Regina at 6:00 a.m. on the 29th day of August 1972 was estimated by interpolating data from the 1200 GMT upper-air charts available for the same day. Temperatures of 60°F and 61°F were reported at Regina at 6 and 7 a.m., respectively. A tephigram may be plotted to show the upper-air structure using 24°C at 850 mb, 11°C at 700 mb and -10°C at 500 mb along with the surface temperature of 60 to 61°F. Regina's elevation is 1884 ft.

The moisture content of the air was low, with dew-point temperatures staying constant in the low to mid forties. A 14% relative humidity was reported during the afternoon.

Regina and Moose Jaw both reached 100°F during the afternoon following the mirage. These were new record high temperatures for the date. Regina had not experienced a 100-degree reading since the 26th day of July 1959, some thirteen years previous.

Early morning mirages happen fairly often at Regina both during hot spells in summer and cold spells in winter. They occur when there is a strong inversion in the lower levels of the atmosphere. Some are more intense than others. In order to photograph a mirage near dawn a camera cannot always be hand-held as the light is quite poor. They are also hard to catch with the camera because of their fleeting nature.

ANNOUNCEMENT

Recent Publication – Meteorological Challenges: A History

Twelve distinguished international scientists participated during October, 1971 in a symposium to mark the opening of the new Headquarters building of the Atmospheric Environment Service at Toronto. (See report in *Atmosphere*, 10, 27–31.) "Meteorological Challenges: A History" (D.P. McIntyre, ed.) has been published to record the thoughts of each speaker who reviewed his own field of meteorological interest. The book is not a mere transcript of a number of

Continued on page 36

BOOK REVIEWS

CLOUDS OF THE WORLD — A COMPLETE COLOUR ENCYCLOPEDIA. By Richard Scorer, David and Charles, Newton Abbot, 1972, 176 pp., 47 diagrams, 369 photographs, £12.60.

Here is truly a book for everyone. The combination of breathtakingly beautiful colour photographs and superb colour reproduction would make this volume a useful addition to the libraries of book and art connoisseurs and of professional and amateur photographers. Professional and amateur students of weather and of meteorology will find in the text material accompanying the photographs an exciting and comprehensive course on atmospheric dynamics, cloud and precipitation physics, atmospheric optics and synoptic meteorology. As an encyclopedia of weather phenomena and cloud forms, this book would be invaluable for school libraries — as reference material for both teachers and students.

Meteorologists will naturally wish to know how this book differs from the W.M.O. Cloud Atlas. Fundamentally, its purpose is totally different; it is not designed to facilitate codification or recognition of obscure sub-species, but to facilitate comprehension of the physical processes associated with visible atmospheric phenomena of all types. This volume covers all such phenomena, and to that extent is not restricted to clouds alone, and in addition has a deliberately broad geographic coverage for its illustrations, permitting an appreciation of climate and climatic processes all over the world. In its technical content, *Clouds of the World* departs significantly from the W.M.O. Cloud Atlas. The text material details mechanisms rather than structure, but the chief difference lies in the photographs. These are almost exclusively in colour, and many were not taken by surface observers. In addition to radar and aircraft photographs, there are numerous shots from both manned and unmanned satellites. A number are presented in stereo format, and there is an appendix dealing with photogrammetry and stereophotography.

A good idea of the subjects covered in this book can be obtained from the following list of section headings:

- | | |
|--------------------------------|-----------------------------------|
| 1. Cumulus | 2. Glaciation of Convection Cloud |
| 1.1 Thermals and small cumulus | 2.1 Cumulus and stratocumulus |
| 1.2 Pileus | 2.2 Glaciated Anvils |
| 1.3 Streets | 2.3 Anvil plumes |
| 1.4 Castellatus | 2.4 Ice fallout |
| 1.5 Warm rain | |
| 1.6 Anvils and stratocumulus | |
| 3. Showers | 4. Cirrus |
| 3.1 Waves and downdrafts | 4.1 Fibrous patches |
| 3.2 Scud | 4.2 Extensive cirrus |
| 3.3 Squalls | 4.3 Falling cirrus |
| 3.4 Cold fronts | |
| 3.5 Cold lows | |
| 3.6 Mamma | |

- | | |
|--|--|
| <ul style="list-style-type: none"> 5. Wave Clouds <ul style="list-style-type: none"> 5.1 Mountain waves 5.2 Wave holes 5.3 Lee waves 5.4 Glaciation in waves 5.5 Castellatus in waves 5.6 Unsteady waves 5.7 Separation 5.8 Wave cloud recognition 5.9 Billows in waves
 7. Altcumulus <ul style="list-style-type: none"> 7.1 Upward growth 7.2 Cellular growth 7.3 Radiative effects 7.4 Glaciation of altocumulus
 9. Fog and Inversions <ul style="list-style-type: none"> 9.1 Radiation fog 9.2 Valley inversions 9.3 Sea fog 9.4 Steaming fog 9.5 The tropopause
 11. Condensation Trails <ul style="list-style-type: none"> 11.1 Cloud close to the aircraft 11.2 Exhaust trails in aircraft wake 11.3 Contrail shadows 11.4 Glaciation and distortion
 13. Optical Phenomena <ul style="list-style-type: none"> 13.1 Surround of observer's shadow 13.2 Water droplet arcs 13.3 Ice crystal arcs 13.4 Illumination effects 13.5 Refraction in air 13.6 Polarisation | <ul style="list-style-type: none"> 6. Billows <ul style="list-style-type: none"> 6.1 Billows in waves 6.2 Billows in layers 6.3 Complex structure 6.4 Rolls and ground billows 6.5 Cirrus billows
 8. Warm Sector Cloud <ul style="list-style-type: none"> 8.1 Sea fog 8.2 Low stratus 8.3 Damp air and ground
 10. White Plumes <ul style="list-style-type: none"> 10.1 Water-laden plumes 10.2 Other white plumes
 12. Droplets and Windblown Material <ul style="list-style-type: none"> 12.1 Captured ice 12.2 Water droplets 12.3 Windblown material
 14. Rotation <ul style="list-style-type: none"> 14.1 Dust devils 14.2 Cloud layer vortices 14.3 Waterspouts and tornadoes 14.4 Tropical cyclones |
|--|--|

The above prosaic listing conveys in part the great depth of the subject matter, and indicates the wide spectrum of uses to which this major reference work could be put by atmospheric scientists. The only problem posed by this volume of lasting value and beauty is whether to put it in one's office, one's den or one's living room.

W.L. Godson
Atmospheric Environment Service
Toronto

one-hour discourses but includes a richer amount of material which only a printed publication can contain.

Topics covered by authors are: The General Circulation of the Atmosphere, J. Smagorinsky; Radiation in the Atmosphere, F. Möller; The Physics of Clouds and Precipitation, B.J. Mason; Upper Atmosphere Meteorology, R.J. Murgatroyd; The Acquisition of Meteorological Data, V.E. Suomi; Dynamic Weather Prediction, G.P. Cressman; Small-Scale Motions, J. Clodman; Atmospheric Chemistry and Environmental Pollution, B. Bolin; Atmospheric Boundary Layer, R.W. Stewart; Applied Meteorology and Environmental Utilization, R.E. Munn; The First Century of the Meteorological Service of Canada, P.D. McTaggart-Cowan; Winds of Change, R.M. White.

The book is available at a cost of \$10.00 by mail from Information Canada, Ottawa; also at Information Canada bookshops or through booksellers (Catalogue No. En56-4172).

MEMBERSHIP APPLICATION FORM

(Please write in Block Letters)

General SURNAME
OR
Student GIVEN NAMES
Member PERMANENT ADDRESS

TITLE, RANK, DECORATIONS, DEGREES OR PROFESSIONAL
QUALIFICATIONS

OCCUPATION
(for record purposes only; if student, indicate university and year
studies will be completed)

Sustaining NAME OR AGENCY
Member BUSINESS ADDRESS

Membership Please enroll me as a member of the
Status Canadian Meteorological Society effective January 1, 19....., to
Required receive all publications issued by the Society from that date. I
attach a cheque for \$ payable to the *Canadian Meteorological Society*.

Signature of Applicant

Mail completed application forms to:
Corresponding Secretary
Canadian Meteorological Society
P.O. Box 41, Willowdale, Ontario
M2N 5S7.

CMS dues for 1973:
General Member \$15.00
Student Member \$ 5.00
Sustaining Member \$50.00 (min.)

INFORMATION FOR AUTHORS

Articles may be contributed either in the English or French language. Authors need not be members of the Canadian Meteorological Society. Manuscripts for *Atmosphere* should be sent to the Editor, *Atmosphere*, P.O. Box 41, Willowdale, Ontario M2N 5S7. After papers have been accepted for publication, authors will receive galley proofs along with reprint order forms.

Manuscripts should be submitted in duplicate, typewritten with double-spacing and wide margins. Headings and sub-headings should be clearly designated. A concise, relevant and substantial abstract is required.

Tables should be prepared on separate sheets, each with concise headings.

Figures should be provided in the form of two copies of an original which should be retained by the author for later revision if required. A list of legends should be typed separately. Labelling should be made in generous size so that characters after reduction are easy to read. Line drawings should be drafted with India ink at least twice the final size on white paper or tracing cloth. Photographs (halftones) should be glossy prints at least twice the final size.

Units. The International System (SI) of metric units is preferred. Units should be abbreviated only if accompanied by numerals, e.g., '10 m', but 'several metres.'

Footnotes to the text should be avoided.

Literature citations should be indicated in the text by author and date. The list of references should be arranged alphabetically by author, and chronologically for each author, if necessary.

Italics should be indicated by a single underline.

RENSEIGNEMENTS POUR LES AUTEURS

Les **articles** peuvent être soumis en anglais ou en français. Les auteurs peuvent être membres ou non de la Société météorologique du Canada. Les manuscrits pour *Atmosphère* doivent être envoyés à: le Rédacteur, *Atmosphère*, C.P. 41, Willowdale, Ontario, M2N 5S7. Une fois les articles acceptés pour publication, les auteurs en recevront des épreuves de même que des formules de commande de copies supplémentaires.

Les **manuscrits** pour *Atmosphère* doivent être en duplicata, dactylographiés en doubles interlignes avec de larges marges. Les titres et sous-titres doivent être clairement indiqués. Chaque article doit comporter un résumé qui soit concis, pertinent et substantiel.

Les **tableaux** doivent être préparés et présentés séparément accompagnés d'un titre et d'un numéro explicatifs concis.

Les **graphiques** doivent être présentés en deux copies dont les originaux devraient être conservés par l'auteur au cas où ils seraient nécessaire de les reviser. Une liste des légendes des graphiques doit être dactylographiée séparément. L'étiquetage doit être de grand format de façon à ce qu'il soit facilement lisible après réduction du format. Le traçage des lignes doit s'effectuer au moyen d'encre de chine en doublant, au moins, le format final, le tout sur papier blanc ou sur papier à calquer et identifié adéquatement. Les photographies (demi-teintes) devraient être présentées sur épreuves glacées au double du format final.

Les **unités.** Le Système International (SI) d'unités métriques est préférable. Les unités devraient être abrégées seulement lorsqu'elles sont accompagnées de nombres, ex: "10m", mais "plusieurs mètres".

Les **notes de renvoi** au texte doivent être évitées.

Les **citations littéraires** doivent être indiquées dans le texte selon l'auteur et la date. La liste des références doit être présentée dans l'ordre alphabétique, par auteur et, si nécessaire, dans l'ordre chronologique pour chaque auteur.

Les **italiques** doivent être indiqués en soulignant les expressions désirées une seule fois.

The Canadian Meteorological Society / La Société Météorologique du Canada

The Canadian Meteorological Society came into being on January 1, 1967, replacing the Canadian Branch of the Royal Meteorological Society, which had been established in 1940. The Society exists for the advancement of Meteorology, and membership is open to persons and organizations having an interest in Meteorology. At nine local centres of the Society, meetings are held on subjects of meteorological interest. *Atmosphère* as the official publication of the CMS is distributed free to all members. Each spring an annual congress is convened to serve as the National Meteorological Congress.

Correspondence regarding Society affairs should be directed to the Corresponding Secretary, Canadian Meteorological Society, P.O. Box 41, Willowdale, Ontario M2N 5S7.

There are three types of membership – Member, Student Member and Sustaining Member. For 1973 the dues are \$15.00, \$5.00 and \$50.00 (min.), respectively. The annual Institutional subscription rate for *Atmosphère* is \$10.00.

Correspondence relating to CMS membership or to institutional subscriptions should be directed to the University of Toronto Press, Journals Department, Front Campus, Toronto, Ontario, Canada M5S 1A6. Cheques should be made payable to the University of Toronto Press.

La Société météorologique du Canada a été fondée le 1^{er} janvier 1967, en remplacement de la Division canadienne de la Société royale de météorologie, établie en 1940. Cette société existe pour le progrès de la météorologie et toute personne ou organisation qui s'intéresse à la météorologie peut en faire partie. Aux neuf centres locaux de la Société, on peut y faire des conférences sur divers sujets d'intérêt météorologique. *Atmosphère*, la revue officielle de la SMC, est distribuée gratuitement à tous les membres. À chaque printemps, la Société organise un congrès qui sert de Congrès national de météorologie.

Toute correspondance concernant les activités de la Société devrait être adressée au Secrétaire-correspondant, Société météorologique du Canada, C.P. 41, Willowdale, Ontario, M2N 5S7.

Il y a trois types de membres: Membre, Membre-étudiant, et Membre de soutien. La cotisation est, pour 1973, de \$15.00, \$5.00 et \$50.00 (min.) respectivement. Les Institutions peuvent souscrire à *Atmosphère* au coût de \$10.00 par année.

La correspondance concernant les souscriptions au SMC ou les souscriptions des institutions doit être envoyée aux Presses de l'Université de Toronto, Département des périodiques, Campus Front, Toronto, Ontario, Canada, M5S 1A6. Les chèques doivent être payables aux Presses de l'Université de Toronto.

Council / Conseil de Administration: 1972-73

<i>President/Président</i>	– G.A. McKay	<i>Councillors-at-large/ Conseillers</i>
<i>Vice-President/Vice-Président</i>	– W.F. Hitschfeld	S.J. Buckler
<i>Past President/Président sortant</i>	– C.M. Penner	J.F. Derome
<i>Corresponding Secretary/ Secrétaire-correspondant</i>	– G.A. McPherson	L.E. Parent
<i>Treasurer/Trésorier</i>	– M.S. Webb	<i>Chairmen of Local Centres/ Présidents des centres</i>
<i>Recording Secretary/ Secrétaire d'assemblée</i>	– C.B. Adamson	

ATMOSPHERE

<i>Editorial Committee/ Comité de rédaction</i>	<i>Associate Editors/Rédacteurs associés</i>	
E.J. Truhlar, <i>Editor-in-Chief/ Rédacteur-en-Chef</i>	B.W. Boville	G.A. McPherson
J.A.W. McCulloch	C. East	J.G. Potter
R.E. Munn	K.D. Hage	V.R. Turner
	J.V. Iribarne	
<i>Editorial Staff/Equipe de rédaction</i>	– N. MacPhail	– A.W. Smith
	– J. Rogalsky, <i>Advertising/Publicité</i>	
<i>Sustaining Member/Membre de soutien</i>	– Air Canada	